JOURNAL OF SYNCHROTRON RADIATION

Volume 22 (2015)

Supporting information for article:

Muffin-tin potentials in EXAFS analysis

B. Ravel

1 Supplemental materials: Muffin tin potentials in EXAFS analysis

1.1 XANES data for $LaNiO_3$ and NiO

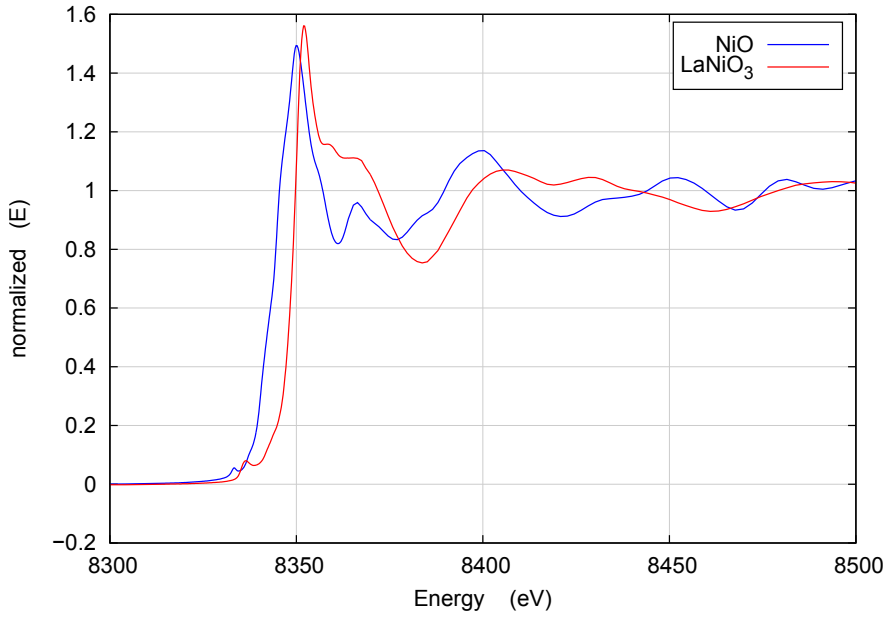

Figure 1: XANES data for NiO (blue) and $LaNiO_3$ (red).

1.2 $LaNiO_3$ phase purity

X-ray powder diffraction data were acquired in θ-2θ mode with a Bruker D2 Phaser[1], operating with Cu Kα radiation and a Lynxeye position sensitive detector (a Ni filter was used to remove Cu Kβ radiation). The angular range was $20° < 2\theta < 80°$, with a step size of 0.02° and a count time of 2 seconds per step.

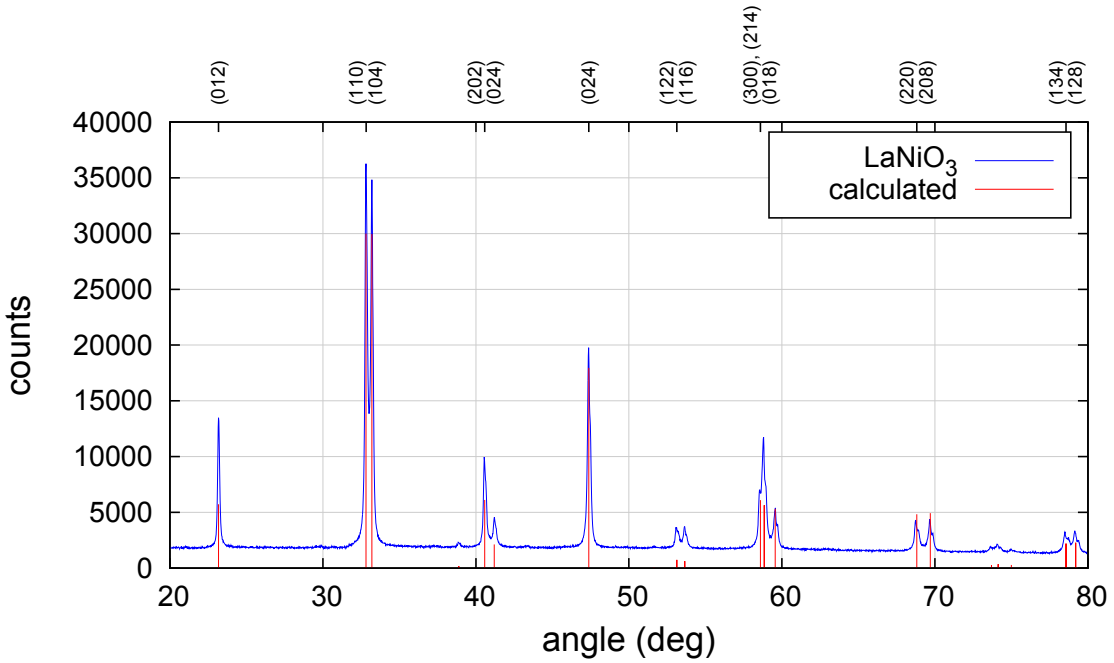

Figure 2: Diffractogram of the $LaNiO_3$ sample compared with peak positions and intensities computed from the known crystal structure.

[1]Any mention of commercial products is for information only; it does not imply recommendation or endorsement by NIST.

1.3 NiO sample preparation

Polycrystalline NiO was prepared by the same method as described in the main text for $LaNiO_3$. To achieve similar particle size, we started with 0.01 mmol of $Ni(CH_3CO_2)_2{\cdot}4H2O$ dissolved in 10 ml of deionised water with the addition of 0.02 mmol of citric acid monohydrate. X-ray powder diffraction demonstrated formation of single phase NiO (olive green) after heating the amorphous precursors at 900° C for 36 hours under flowing oxygen. The mean particle size of the NiO powder was estimated as 2.0 μm by scanning electron microscopy.

A sample of NiO was prepared for X-ray Absorption Spectroscopy (XAS) measurements by dispersing enough fine powder in polyethylene glycol to make an edge step around 0.5. A pellet was then formed in an hydraulic press.

1.4 Analysis of the NiO EXAFS data

NiO is halite structured and analyzed to a radial distance which includes the first four coordination shells. The variables in this fit included parameters for S_0^2, E_0, an isotropic lattice expansion coefficient α, and σ^2 parameters for each of the four single scattering paths. Various multiple scattering paths were included in the fit and parameterized without introducing new variables to the fit.

S_0^2	0.70(5)
E_0	−0.79(55)
α	0.0013(15)
σ^2 – O, 1^{st} shell	0.00476(126)
σ^2 – Ni, 2^{nd} shell	0.00539(56)
σ^2 – O, 3^{rd} shell	0.03217(2058)
σ^2 – Ni, 4^{th} shell	0.00713(95)

Table 1: Results of fit to NiO using the cubic halite model. The unit of E_0 is eV and of σ^2 is Å^2.

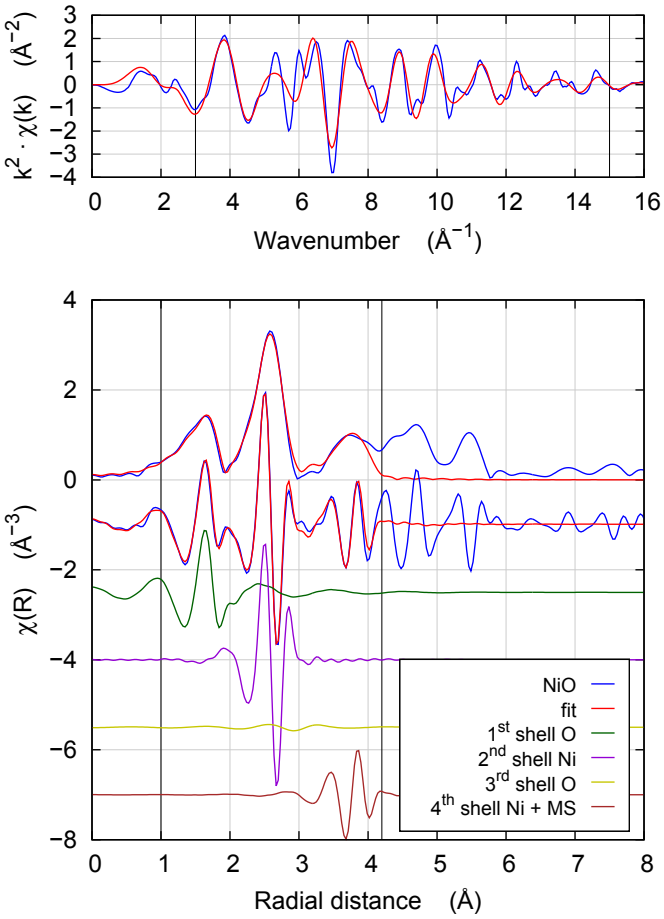

Figure 3: Fit to NiO using the cubic halite structure. The brown line includes the contribution from the fourth shell Ni scatterer plus several collinear MS paths at the same distance. The vertical lines show the ranges of the Fourier transform in k and the fit in R.

1.5 $LaNiO_3$ fit using the constructed Ni SS path

Upon addition of the Ni SS path (brown line in Fig. 4), the fit improved statistically. The R-factor reduced from 0.023 to 0.020. The inclusion of the Ni SS path added 2 floating parameters, taking the fit from 6 to 8 parameters and reducing the freedom ν of the fit from about 15 to about 13. The reduced chi-square χ^2_ν went from 576 to 533 upon addition of the Ni SS path. See Table 1 in the main text.

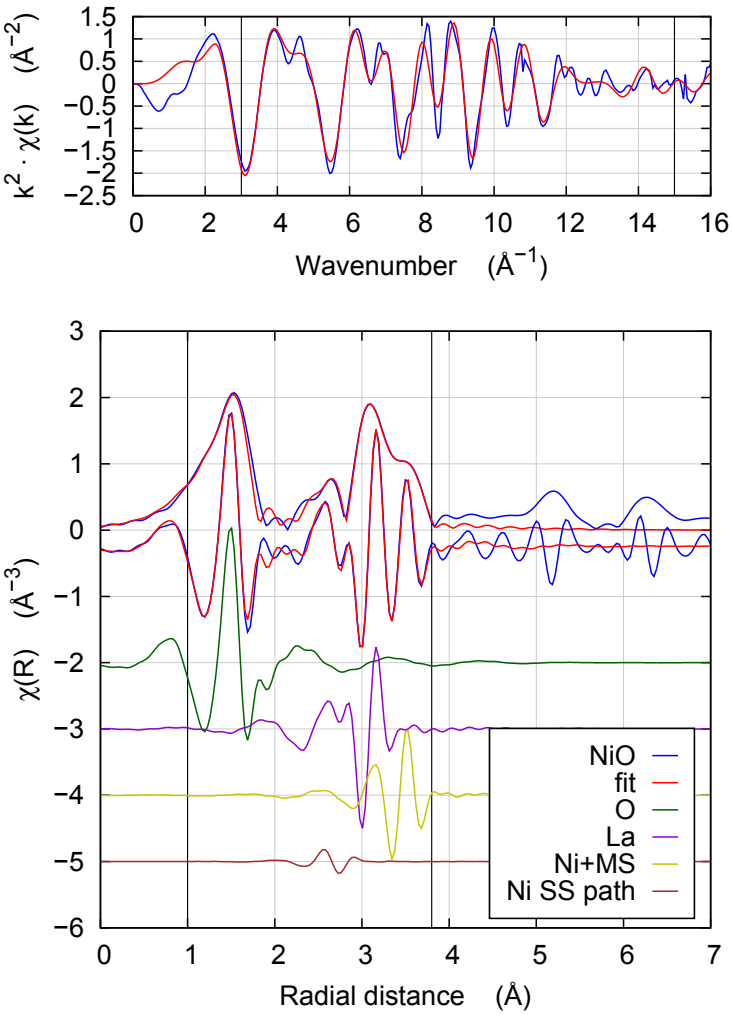

Figure 4: Fit to $LaNiO_3$ using the constructed Ni SS path. The yellow line includes contributions from the third shell Ni scatterer plus several multiple scattering paths at the same path length. The brown line is the Ni SS path added to represent the contribution from the non-diffracting Ni oxide. The vertical lines show the ranges of the Fourier transform in k and the fit in R.

1.6 $LaNiO_3$ fit using the Ni path from NiO

The figure below shows the same fit as in Sec. 1.5 of this supplemental document excpet that the Ni scatterer at about 3 Åis repesented in the fit by the 2^{nd} shell Ni scatterer from NiO. The R-factor here is 0.020 and the reduced chi-square χ^2_ν is 531, both equivalent to the fit with the Ni SS path shown in Sec. 1.5. The number of Ni atoms in the poorly-diffracting NiO phase determined from this fit is 6.8(4.0)% and their R is 3.000(35) Å, both consistent with the results given in the main text.

On visual inspection, this fitting result is indistinguishable from the result shown in Sec. 1.5 using the Ni SS path.

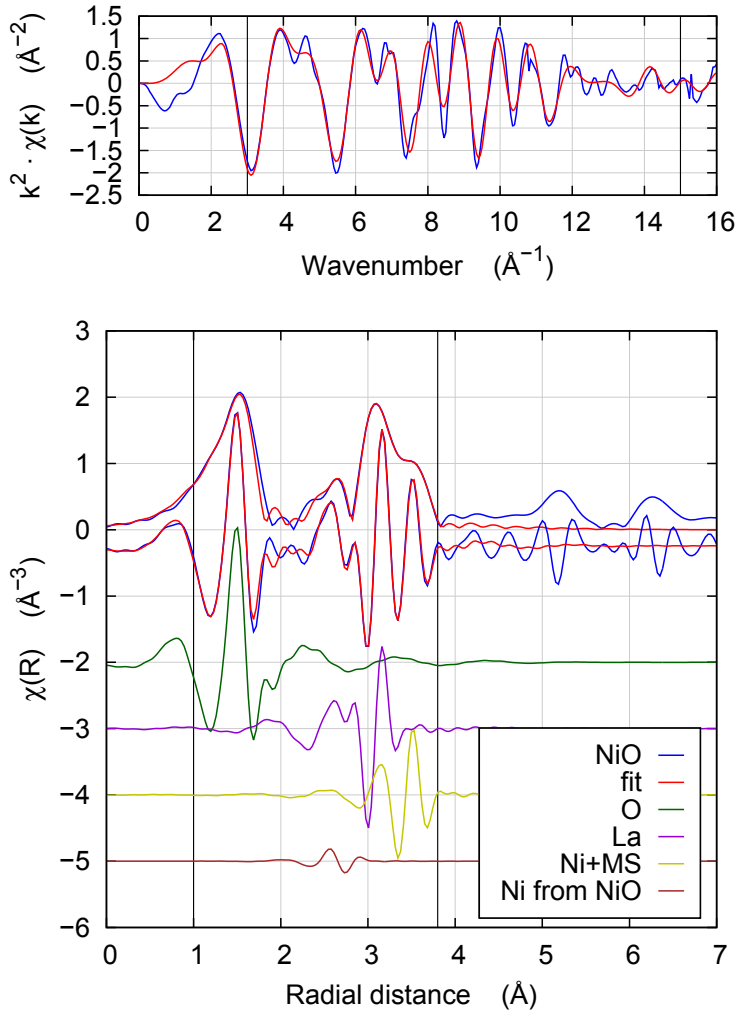

Figure 5: Fit to $LaNiO_3$ using the 2^{nd} shell Ni path from NiO. The yellow line includes contributions from the third shell Ni scatterer plus several multiple scattering paths at the same path length. The brown line is the 2^{nd} shell Ni path from NiO used to account for the non-diffracting Ni oxide. The vertical lines show the ranges of the Fourier transform in k and the fit in R.